

Infrared surface-wave interferometry on W(100)

L. M. Hanssen, D. M. Riffe, and A. J. Sievers

Laboratory of Atomic and Solid State Physics and Materials Science Center, Cornell University, Ithaca, New York 14853-2501

Received August 11, 1986; accepted September 25, 1986

An IR grating on a clean W(100) surface is shown to generate both homogeneous and inhomogeneous surface electromagnetic waves. An observed interference between these two components, which can be described in terms of a two-beam interferometer with variable arm amplitude and fixed optical path, is used to measure the plasma frequency accurately in the IR.

The attenuation of surface electromagnetic waves (SEW's) propagating on a clean W(100) surface has been used to monitor adsorbate vibrational modes,¹ surface reconstruction,² and chemisorption-induced³ changes in the free-carrier behavior of the metal in the room-temperature regime. We report on the measured properties of SEW's at elevated temperatures. At temperatures greater than 1000 K the SEW signal is attenuated to such a large extent that low-intensity surface skimming plane electromagnetic waves (PEW's), which are also generated at the grating coupler, can be detected. Since both kinds of wave are generated coherently at the input but travel across the surface with different velocities, interferometry is possible. This interferometer has been used to measure the plasma frequency of W in the 10- μm wavelength region.

A description of the experimental apparatus and procedures for making SEW attenuation measurements in ultrahigh-vacuum UHV conditions has been given in Ref. 2. Because the SEW wave vector is greater than that of light, gratings etched into the surface are used to couple CO₂ laser radiation into and out of the SEW spectrum.

To identify the interference signature between SEW's and PEW's, the temperature dependence of the signal from the output coupler is measured at many laser frequencies across the ranges of the ¹²CO₂ and ¹³CO₂ laser gases. Each of the eight data traces shown in Fig. 1 represents an intensity-versus-temperature run at a fixed frequency. Note the strong minimum in log (intensity) that occurs near $T = 400^\circ\text{C}$ and $\bar{\nu} = 1000\text{ cm}^{-1}$. For all frequencies the temperature dependence at low temperatures agrees with that calculated for SEW's from the temperature dependence of the dc resistivity $\rho(T)$, namely,

$$I_S(T) = I_{0S} \exp[-\omega^2 L \rho(T) / 4\pi c], \quad (1)$$

where ω is the angular frequency, L the propagation distance, and c the velocity of light. For high temperatures an additional component, which tracks the SEW intensity when the laser's beam angle, input power, or polarization is changed, comes from PEW's generated at the input grating.

Next it is shown that the phase difference between SEW's and PEW's in the IR is large enough over the

sample length to account for the interference effect. The difference in phase between the two beams can be written as

$$\theta = q_S L - q_P L + \phi, \quad (2)$$

where q_S is the SEW wave vector, q_P the PEW wave vector, and ϕ the phase shift between the two waves, which is assumed to be a constant over the frequency region of interest. For a Drude metal in the 10- μm -wavelength region

$$q_S \approx (\omega/c) [1 + \omega^2 / 2\omega_p^2 + (\epsilon_0 + 3/4)(1 - 1/\omega^2 \tau^2) \omega^4 / 2\omega_p^4], \quad (3)$$

where ω_p is the plasma frequency in the IR and ϵ_0 the low-frequency contribution to the dielectric constant from the interband transitions. Since the most effective PEW's are those within a wavelength of the surface at the output coupler, $q_P = \omega/c$; hence the phase difference between the two arms for a Drude metal is

$$\theta \approx (\omega L/c) (\omega^2 / 2\omega_p^2) + \phi. \quad (4)$$

The resultant intensity at the detector now takes on a familiar form, namely,

$$I = I_S + I_P + 2(I_S I_P)^{1/2} \cos \theta. \quad (5)$$

Destructive interference occurs when $\theta = (2n + 1)\pi$, with n a nonnegative integer, and the largest effect appears when the two arms of the optical bridge are balanced. A temperature sweep at a fixed laser frequency (the data shown in Fig. 1) corresponds to varying the relative amplitudes for the two components of Eq. (5) while keeping θ fixed.

To obtain accurate values for $\theta(\omega)$ each data set must be fitted to Eq. (5), so knowledge of the expected temperature and frequency dependences of I_S and I_P is required. The SEW intensity dependence is given in Eq. (1). Although an accurate expression for the PEW intensity dependence requires the solution of a deep grating diffraction problem, we show here that the appropriate temperature-dependent form can be constructed from a simple phenomenological model.

We assume that the near fields at the source that evolve into interfering PEW's and SEW's extend a distance δ_0 above the grating and that the mean SEW amplitude height is a measure of this range. Now

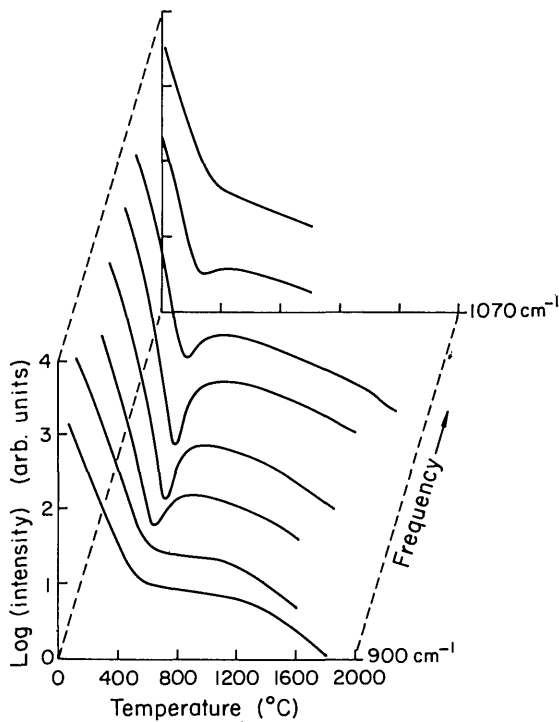


Fig. 1. Transmitted IR intensity as a function of temperature and frequency. Eight SEW signal-versus-temperature scans are shown at approximately equal frequency intervals across the CO₂ laser spectrum.

consider a PEW traveling along the sample surface. In analogy with a parallel-plate transmission line geometry for fixed plate separation δ_0 , the transmitted intensity would be

$$I_P = I_{0P} \exp(-2ry/\delta_0), \quad (6)$$

where r is the normalized real part of the surface impedance of the metal² and y the distance along the surface.

Because of diffraction the height of the PEW actually changes with distance from the source; hence from the geometry

$$\delta(y) = \delta_0 + y \tan(\alpha), \quad (7)$$

where δ_0 is the height at $y = 0$ and $\alpha = \sin^{-1}(\lambda/\delta_0)$, the angle to the first minimum in a single-slit diffraction pattern. The appropriate generalization of Eq. (6) is

$$I_P = I_{0P} \exp\left\{-\int dy [2r/\delta(y)]\right\}. \quad (8)$$

Another loss mechanism for this component occurs at the output coupler, $y = L$, since only the fraction $[\delta_0/\delta(L)]$ of the PEW will be coupled out to the detector. The resultant expression is

$$I_P = I_{0P}(1 + fL/\delta_0)^{-(1+2r/f)}, \quad (9)$$

where

$$f = \lambda/(\delta_0^2 - \lambda^2)^{1/2}. \quad (10)$$

Three adjustable parameters θ , I_{0S} , and I_{0P} in Eqs. (1), (5), and (9) are used to fit the temperature-dependent data with the data near $I_S \approx I_P$ weighted most heavily. Figure 2 shows three data sets with the corre-

sponding best fit given by this model. The destructive interference between the SEW's and the PEW's increases in strength as the laser frequency is decreased from 1072 cm⁻¹ [Fig. 2(a)] to 995 cm⁻¹ [Fig. 2(c)]. Sample movement produces the high-temperature difference between the data and the model shown in Figs. 3(b) and 3(c). The fits show that the PEW intensity at room temperature is $\sim 1\%$ of the SEW value. Even here the PEW component cannot be neglected since at frequencies where a π phase shift occurs the resultant intensity is $\sim 20\%$ smaller than for the SEW component alone.

In order to compare the results with relation (3) the measured phase angle θ is plotted against the frequency cubed as shown in Fig. 3. A linear dependence is observed over the measured range covering nearly π rad. A least-squares fit to these data gives $L/(2c\omega_p^2) = 1.04(\pm 0.04) \times 10^{25} \text{ sec}^{-3}$ and $\phi = -0.51(\pm 0.05)\pi$.

Our measurements show that the output coupling of both the SEW's and the PEW's takes place over the full extent of the 3.8-mm-wide output grating, so half of this distance is added to the separation between gratings to obtain the total propagation distance.

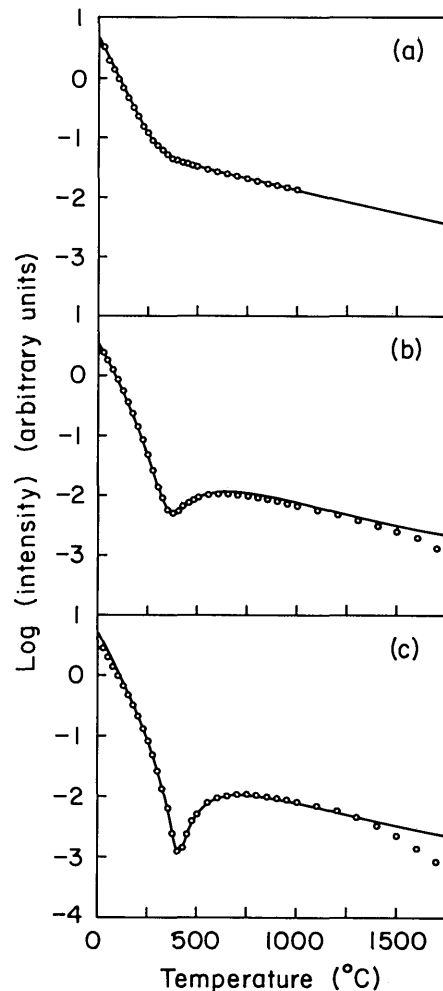


Fig. 2. Comparison of three sets of data with the two-beam interferometer model. The open circles represent the data and the solid line the model fit. The three frequencies are (a) 1072 cm⁻¹, (b) 1027 cm⁻¹, and (c) 995 cm⁻¹.

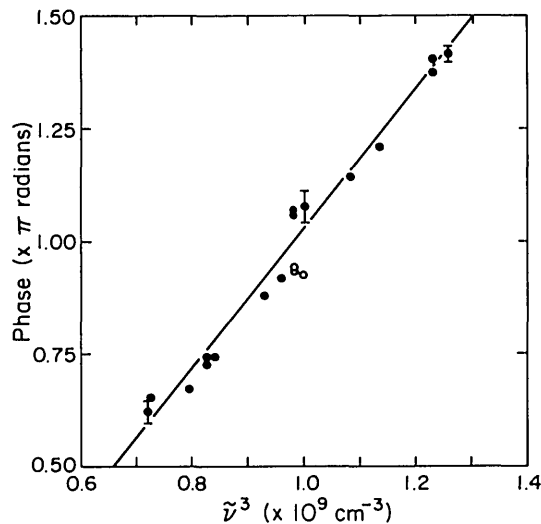


Fig. 3. Frequency dependence of the phase difference between the two arms of the interferometer. The filled circles represent the data; the open circles are alternative values for the data points directly above them [since $\cos(\pi + x) = \cos(\pi - x)$]. The solid line shows a linear least-squares fit.

Substitution of $L = 4.94$ cm gives $\hbar\omega_p = 7.0(\pm 0.3)$ eV for the plasma frequency in the IR.

By measuring the transmitted intensity as a function of placement of the input beam on the input grating, it has been possible to show that the PEW's occur not because of the impedance change at the grating-smooth-metal boundary⁴ but instead because of the finite number of grating lines intercepted by the input beam (about 20 in the actual experiment). For a plane wave incident upon an infinite grating at the angle for maximum SEW generation the first-order PEW beam is forbidden, but when the grating consists of a small number of lines this selection rule against the first-order beam is weakened, so some PEW's do appear. The end result is that a narrow grating coupler or a small spot size automatically sends PEW's along with the desired SEW's across the surface.

Another feature of our data that needs examination is the finite intensity at the destructive interference condition. At a frequency near 1000 cm^{-1} , where $\theta = \pi$, the resultant intensity should dip down to the background-noise level when $I_S = I_P$; however, the smallest measured value is $\sim 4\%$ of the SEW (or PEW) value at that temperature. [This is for the data at 995 cm^{-1} shown in 2(c).] There are two contributions to this 4% minimum. The first is that the SEW beam is attenuated more strongly than the PEW beam along the deep grating couplers. This leads to less than complete destructive interference since the two components' intensities cannot be matched across the entire length of the output coupler (and hence across all the detector). The second contribution comes from the difference in SEW and PEW wave vectors. This difference in wave vector (which causes the whole interference effect in the first place) also leads to less than complete destructive interference since the phase angle θ is not a constant across the whole output coupler. From measured values of the difference in attenuation and wave vector of the two components we calculate minimum I/I

I_S (or I/I_P) $\approx 2.5\%$, in reasonable agreement with the measured value of 4%.

The experimentally determined value of the constant phase factor $\phi = -\pi/2$ cannot be explained within the framework of this simple phenomenological picture. A rigorous diffraction calculation may be required for the relative phases of the two components at the input and output coupler to be explored.

Our direct determination of the real part of the inverse dielectric function of a clean W(100) surface that we have characterized with an effective plasma frequency ($\hbar\omega_p = 7.0$ eV) in the Drude model approximation can be compared with the value deduced for the same frequency region from reflectivity⁵ and ellipsometric⁶ measurements ($\hbar\omega_p = 6.4$ eV).⁷ The errors in these earlier measurements are large enough that the two values are within the uncertainties.

This new measurement technique is not limited to W. From relation (4) the criterion for destructive interference (assuming that $\phi = -\pi/2$) can be rewritten in terms of the SEW attenuation coefficient in Eq. (1) to give

$$\omega^2 L \rho(T) / 4\pi c = 3\pi / \omega \tau. \quad (11)$$

Inspection of the right-hand side of this expression shows that the IR frequency should be chosen to ensure that $\omega \tau > 1$ for a particular metal so that the attenuation of the SEW will not obscure the interference effect.

The analysis given here, which uses the interference between SEW's and PEW's to determine the plasma frequency of the metal, should have general applicability in the IR. Moreover, to produce such an effect gratings are not required, since the interference has already been detected with an aperture-excitation technique⁸ on a smooth metal surface.

Discussions with J. J. Quinn, V. A. Yakovlev, and G. Zhizhin by A. J. Sievers have been particularly stimulating. This research is supported by the National Science Foundation under grant DMR-84-09823 and by the U.S. Air Force Office of Scientific Research under grant AFOSR-85-0175. Additional support has been received from the Materials Science Center (MSC) at Cornell University, MSC Rep. No. 5848.

References

1. D. M. Riffe, L. M. Hanssen, A. J. Sievers, Y. J. Chabal, and S. B. Christman, *Surf. Sci.* **161**, L559 (1985).
2. D. M. Riffe, L. M. Hanssen, and A. J. Sievers, *Phys. Rev. B* **34**, 692 (1986).
3. D. M. Riffe, L. M. Hanssen, and A. J. Sievers, "Infrared observation of adsorbate induced changes in free carrier surface scattering," *Surf. Sci.* (to be published).
4. Z. Schlesinger and A. J. Sievers, *Appl. Phys. Lett.* **36**, 409 (1980).
5. J. H. Weaver, C. G. Olson, and D. W. Lynch, *Phys. Rev. B* **12**, 1293 (1975).
6. L. V. Nomerovanya, M. M. Kirillova, and M. M. Noskov, *Sov. Phys. JETP* **33**, 405 (1971).
7. M. A. Ordal, R. J. Bell, R. W. Alexander, L. L. Long, and M. R. Querry, *Appl. Opt.* **24**, 4493 (1985).
8. M. A. Chesters, S. F. Parker, and V. A. Yakovlev, *Opt. Commun.* **55**, 17 (1985).